http://dx.doi.org/10.5012/bkcs.2014.35.12.3553

Synthesis and Electrochemical Performance of Reduced Graphene Oxide/$AlPO_4$-coated $LiMn_{1.5}Ni_{0.5}O_4$ for Lithium-ion Batteries

Jaehyun Hur and Il Tae Kim*

Department of Chemical and Biological Engineering, Gachon University, Gyeonggi-do 461-701, Korea
**E-mail: itkim@gachon.ac.kr*
Received June 12, 2014, Accepted August 18, 2014

The reduced graphene oxide(rGO)/aluminum phosphate($AlPO_4$)-coated $LiMn_{1.5}Ni_{0.5}O_4$ (LMNO) cathode material has been developed by hydroxide precursor method for LMNO and by a facile solution based process for the coating with GO/$AlPO_4$ on the surface of LMNO, followed by annealing process. The amount of $AlPO_4$ has been varied from 0.5 wt % to 1.0 wt %, while the amount of rGO is maintained at 1.0 wt %. The samples have been characterized by X-ray diffraction, scanning electron microscopy, and high-resolution transmission electron microscopy. The rGO/$AlPO_4$-coated LMNO electrodes exhibit better cyclic performance compared to that of pristine LMNO electrode. Specifically, rGO(1%)/$AlPO_4$(0.5%)- and rGO(1%)/$AlPO_4$(1%)-coated electrodes deliver a discharge capacity of, respectively, 123 mAh g^{-1} and 122 mAh g^{-1} at C/6 rate, with a capacity retention of, respectively, 96% and 98% at 100 cycles. Furthermore, the surface-modified LMNO electrodes demonstrate higher-rate capability. The rGO(1%)/$AlPO_4$(0.5%)-coated LMNO electrode shows the highest rate performance demonstrating a capacity retention of 91% at 10 C rate. The enhanced electrochemical performance can be attributed to (1) the suppression of the direct contact of electrode surface with the electrolyte, resulting in side reactions with the electrolyte due to the high cut-off voltage, and (2) smaller surface resistance and charge transfer resistance, which is confirmed by total polarization resistance and electrochemical impedance spectroscopy.

Key Words : Reduced graphene oxide, Aluminum phosphate, 5 V Spinel, Lithium-ion batteries

Introduction

Lithium-ion batteries have revolutionized the portable electronics industry due to its high energy density with outstanding cyclic performance. However, it still requires carrying out higher energy density for the applications to the power sources in hybrid electric vehicles (HEV) and plug-in hybrid electric vehicles (PHEV).[1] In this regard, since manganese (Mn) and iron (Fe) are environmentally friendly elements as well as inexpensive, $LiMn_2O_4$ (4 V spinel) and $LiFePO_4$ (3.4 V olivine) cathodes have become more attractive, which offer better safety and higher-rate capability compared to the layered oxide cathodes. Nevertheless, they suffer from the limited energy density due to their low capacity and/or operating voltage. Based on this scenario, it has been pursued to obtain enhanced energy and power densities by increasing the operating voltage of spinel cathode materials, while maintaining the excellent rate capability resulting from the three dimensional diffusion of lithium ions in the lattice. In this sense, the cation substitution in $LiMn_{2-x}M_xO_4$ spinel oxide (M = Cr, Co, Fe, and Ni) is the effective way because they can deliver the capacity around a flat operating voltage of ~5 V.[2,3] Among the various 5 V spinel cathodes, $LiMn_{1.5}Ni_{0.5}O_4$ (LMNO) has been attracted due to its high capacity resulting from the operation of $Ni^{2+/3+}$ and $Ni^{3+/4+}$ redox couples,[4,5] which provides higher working voltage than those of commercial cathodes such as $LiMn_2O_4$ (4.1 V), $LiCoO_2$ (3.9 V), and $LiFePO_4$ (3.4 V).[6] However, LMNO reveals poor electrochemical performance. The capacity fading phenomenon is considered to be due to the large lattice strain upon cycling since it involves the formation of three cubic phases with a large lattice parameter difference during the charge/discharge process in addition to the corrosion reaction between the cathode surface and the electrolyte at the high operating voltage of ~5 V.[7-9] Some of the partial substitution of Mn and Ni in LMNO by other elements such as Mg, Cr, Fe, Co, Mo, W, and Tb has been pursued to enhance the electrochemical performance.[10-14]

On the other hand, another effective way to improve the cyclic performance is to modify the electrode surface in order to suppress corrosion reaction between electrode surface and electrolyte.[8,9] The surface modification including conductive agents like carbon and aluminum has been successfully applied to the cathodes, where the formation of conductive coating layers consisting of nanostructured carbon materials leads to improved electronic conductivity, cyclability, and rate capability.[15-17] Based on these approaches, graphene has been considered as an effective conductive coating material due to its outstanding physical properties including high specific surface area, high electronic conductivity, and excellent structural stability.[18,19]

In this study, we report the LMNO cathode material with a conductive hybrid coating layer consisting of reduced graphene oxide (rGO)/aluminum phosphate ($AlPO_4$). The $AlPO_4$ has been widely utilized for the surface modification of cathodes due to its high chemical-resistance.[20] In addition,

$AlPO_4$ could be porous based on the synthesis procedure and help deliver lithium into the cathode. However, it does not have conductive property. By introducing a conductive coating material, rGO, and generating hybrid structure consisting of rGO and $AlPO_4$, the synergetic effect of hybrid coating for LMNO electrode is expected. The surface modification of LMNO active material proceeds by an electrostatic interaction between the coating precursor material and the pristine LMNO material by controlling the pH of the solution. The reduction of graphene oxide is achieved simultaneously during the annealing process for $AlPO_4$ formation in an inert argon atmosphere. The rGO/$AlPO_4$-coated LMNO cathode demonstrates excellent cyclic performance and high-rate capability even at high current rate of 10 C. Therefore, the surface modification with rGO/$AlPO_4$ of pristine LMNO may promise as a viable cathode material for lithium-ion batteries.

Experimental

Materials Synthesis. $LiMn_{1.5}Ni_{0.5}O_4$ (LMNO) powders were synthesized by a hydroxide precursor method. In brief, the precipitation of the hydroxide precursors was prepared from a solution including the required amount of manganese acetate and nickel acetate by adding KOH. After drying the hydroxide precursors, it was fired with a required amount of $LiOH{\cdot}H_2O$ at 900 °C in air for 12 h with a heating and cooling rate of 3 °C min^{-1}.

Graphene oxide (GO) was prepared *via* a modified Hummers method.[21] In brief, graphite powder (2 g) and sodium nitrate ($NaNO_3$;1 g) were mixed in concentrated sulfuric acid (H_2SO_4;96 mL) under stirring and cooled below 20 °C with an ice bath. Under continuous stirring, potassium permanganate ($KMnO_4$;6 g) was added gradually with keeping the solution temperature below 20 °C. Then, the mixture was stirred at 35 °C in an oil bath for 18 h and then 150 mL of DI water was slowly added to the mixture. After dilution with an additional 500 mL of DI water, 30% hydrogen peroxide (H_2O_2; 5 mL) was added to the mixture. After stirring for 2 h, the mixture was filtered and washed with a 10% HCl solution (1000 mL) and then DI water until the pH of the supernatant is neutral. Finally, the resulting sample was dried in a vacuum oven at 70 °C overnight.

For the coating the LMNO surface, required amounts of GO were dispersed in DI water and sonicated for 1 h. Then, an aluminum nitrate nonahydrate ($Al(NO_3)_3{\cdot}9H_2O$) aqueous solution with required molar concentration was added to the GO suspension and sonicated for 2 h. Under stirring, an ammonium phosphate ($(NH_4)_2HPO_4$) aqueous solution was added dropwise to develop $AlPO_4$ nanoparticles on GO sheets. Ammonium hydroxide (NH_4OH) was added to the suspension to increase the pH to 10. The pristine LMNO powder was then added slowly to the colloidal coating solution with stirring, where the electrode surface is negatively-charged and coating material is positively-charged, meaning the electrostatic interaction between electrode surface and coating material.[22] After that, the mixture was filtered and the resulting sample was dried at 120 °C for 8 h. The dried powder was ground and annealed at 400 °C for 5 h under inert argon atmosphere. The rGO content was maintained constant at 1.0 wt % while $AlPO_4$ was varied from 0.5 to 1.0 wt %.

Materials Characterization. The structure of the as-prepared samples was characterized by an X'pert Pro Alpha-1 (wavelength of 1.54 Å) in the range of 10-80° with a scan rate of 0.03° s^{-1}. The morphology, micro/nano structure, and composition of the powder samples were characterized with a JEOL 2010F transmission electron microscope (TEM) and LEO 1530 scanning electron microscope (SEM).

Electrochemical Measurements. Electrochemical performances were assessed with CR2032 coin type cells. The cells were assembled with cathode films, lithium foil anodes, 1 M $LiPF_6$ in a 1:1 (v/v) mixture of ethylene carbonate/diethyl carbonate (EC/DEC) electrolyte, and Celgard polypropylene separator. The cathodes were prepared with the mixture consisting of 80 wt % electrochemically active powders, 10 wt % Super P, and 10 wt % polyvinylidene fluoride (PVDF) in *N*-methyl-2-pyrrolidone (NMP). As-prepared mixtures were then coated onto aluminum foil and dried at 60 °C in an oven for 3 h and then at 120 °C in a vacuum oven overnight. The sample electrodes were punched out of the foil to generate circular electrodes of 1.13 cm^2 area, which gives an active material content of 6-7 mg. All cells were prepared in Ar-filled glove box. The assembled cells were tested in the voltage range of 3.5-5.0 V at a constant current density of C/6 corresponding to 24.5 mA g^{-1} at room temperature. The rate capability was evaluated with a constant charge at C/6 and a sequential increase in the discharge rate from C/6 to 10 C. EIS measurements were carried out with a Solartron 1260A impedance analyzer in the frequency range of 100 kHz to 0.01 Hz with an AC voltage amplitude of 10 mV. Before the EIS measurement, all samples were charged to 50% state of charge (SOC). Li foil served as both the counter and reference electrodes during the EIS measurements.

Results and Discussion

Structural and Morphological Characterizations. Figure 1 shows the XRD patterns of as-prepared LMNO, $AlPO_4$- and rGO/$AlPO_4$-coated LMNO samples. All the reflections could be indexed based on the cubic spinel structure, illustrating that the surface modifications with rGO and $AlPO_4$ do not change the bulk structure of the spinel sample. In addition, the samples show weak diffraction peaks at 37.6°, 43.7°, and 63.5°, as marked with asterisks, which is due to the $Li_xNi_{1-x}O$ impurity phase (PDF No. 01-077-2023) in $LiMn_{1.5}Ni_{0.5}O_4$.

Figure 2 shows the morphology of the synthesized GO, GO/$AlPO_4$ hybrid, and rGO/$AlPO_4$-coated LMNO. The TEM image of GO in Figure 2(a) illustrates the wrinkled morphology, and the inset demonstrates the diffraction pattern, which confirms the well-defined crystalline structure of GO.[23] In the case of GO/$AlPO_4$ coating material as shown in Figure

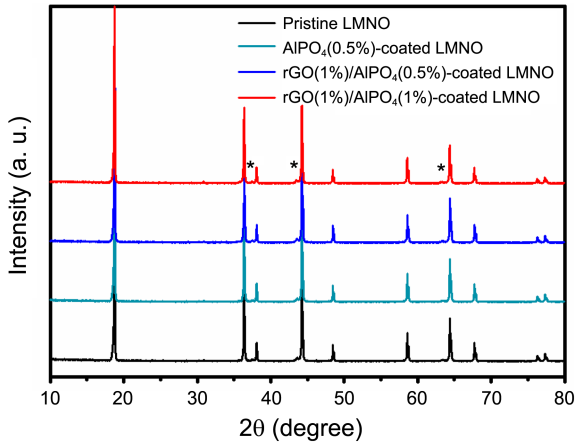

Figure 1. XRD patterns of LiMn$_{1.5}$Ni$_{0.5}$O$_4$ before and after surface modification with AlPO$_4$ and rGO/AlPO$_4$.

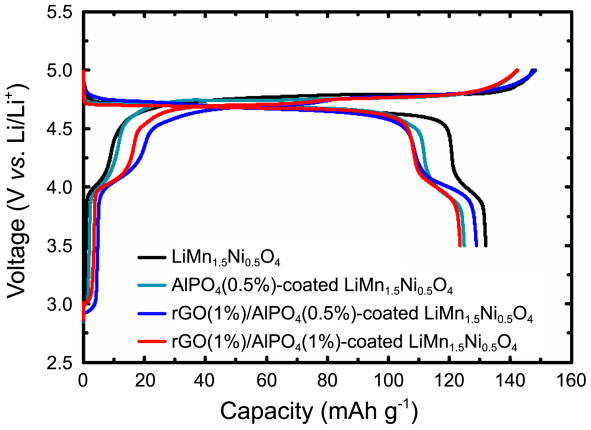

Figure 3. The initial voltage profiles of LiMn$_{1.5}$Ni$_{0.5}$O$_4$ before and after surface modification with AlPO$_4$ and rGO/AlPO$_4$.

2(b), AlPO$_4$ nanoparticles are attached to the surface of graphene oxide, which can be ascribed to the electrostatic interaction between GO surface with negative charge and Al^{3+} with positive charge resulting from the addition of aluminum nitrate nonahydrate ($Al(NO_3)_3{\cdot}9H_2O$) and then the addition of ammonium phosphate ($(NH_4)_2HPO_4$) to generate AlPO$_4$.

Figure 2(c) shows the SEM image of pristine LMNO, and the SEM and TEM images of rGO/AlPO$_4$-coated LMNO are demonstrated in Figure 2(d) and (e). As illustrated in Figure 2(d), after the annealing process, each amorphous AlPO$_4$ nanoparticles on graphene oxide sheet become to form coalesced amorphous regions (blue arrows), resulting in the observation of a few layers of rGO with amorphous regions corresponding to AlPO$_4$. In addition, the rGO/AlPO$_4$ hybrids (outlined with yellow lines) are well-coated on the surface of the LMNO particles. The EDX data confirms that the elements of Al, P, and C in AlPO$_4$ and rGO are homogeneously distributed and coated on the surface of LMNO.

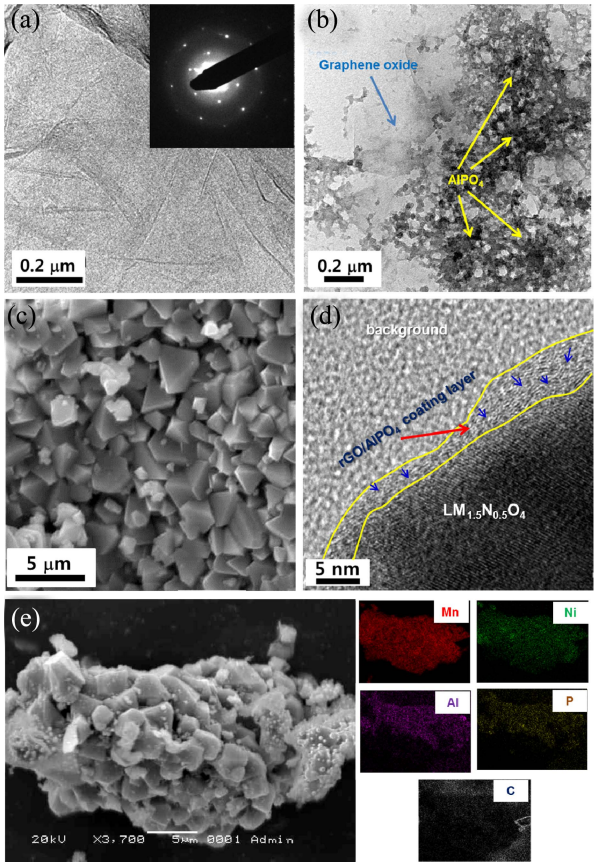

Figure 2. TEM images of (a) GO and (b) GO/AlPO$_4$ hybrid. (c) SEM image of LiMn$_{1.5}$Ni$_{0.5}$O$_4$. (d) TEM and (e) SEM image of rGO/AlPO$_4$-coated LiMn$_{1.5}$Ni$_{0.5}$O$_4$.

Electrochemical Performance. Figure 3 compares the initial charge/discharge voltage profiles of the pristine and surface-modified LMNO samples. The LMNO exhibits a potential plateau at around 4.7 V, which is attributed to the two-step oxidation/reduction of Ni^{2+}/Ni^{3+} and Ni^{3+}/Ni^{4+}, while the short potential plateau at around 4.0 V is ascribed to the redox reaction of Mn^{3+}/Mn^{4+} couples.[24,25] The initial discharge capacity of pristine, AlPO$_4$(0.5%)-, rGO(1%)/AlPO$_4$(0.5%)-, and rGO(1%)/AlPO$_4$(1%)-coated LMNO is 132, 126, 129, and 124 mAh g^{-1}, respectively.

Figure 4 compares the cyclic performances of the pristine and surface-modified LMNO electrodes. The pristine LMNO electrode delivers a capacity of 101 mAh g^{-1} and exhibits a capacity retention of ~77% at 100 cycles. This capacity fade

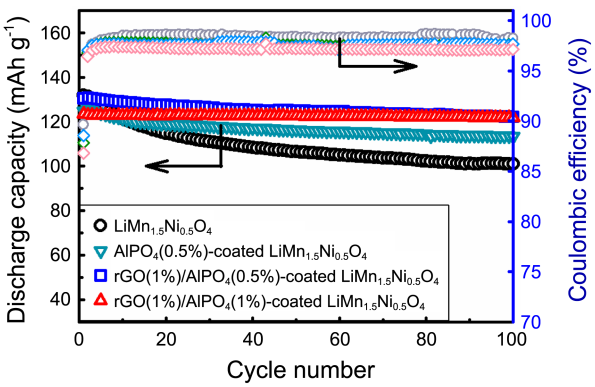

Figure 4. Cyclic performance of LiMn$_{1.5}$Ni$_{0.5}$O$_4$ before and after surface modification with AlPO$_4$ and rGO/AlPO$_4$.

could be a result of side reactions with the electrolyte due to the high cut-off voltage. On the other hand, all the surface-modified LMNO electrodes show better capacity retention than the pristine LMNO electrode. In the case of $AlPO_4$-coated electrode, for instance, it exhibits a capacity retention of 91% at 100 cycles. Furthermore, the rGO(1%)/$AlPO_4$ (0.5%)-coated LMNO delivers a capacity of 123 mAh g^{-1} corresponding to a capacity retention of 96% at 100 cycles, while the rGO(1%)/$AlPO_4$(1%)-coated LMNO exhibits a capacity of 122 mAh g^{-1} and a capacity retention of 98% at the same cycle numbers.

It is noted that the rGO/$AlPO_4$-coated LMNO electrodes demonstrate better cyclic performance compared to $AlPO_4$-coated electrode. The enhanced cyclic performance could be attributed to more conductive property of hybrid coating layer in addition to the suppression of side reactions between electrode and electrolyte at high cut-off voltage. Therefore, it can be concluded that the introduction of rGO/$AlPO_4$ hybrid coating materials is beneficial to obtain enhanced cyclic performance with the LMNO cathodes.

The rGO(1%)/$AlPO_4$(0.5%)-coated LMNO electrode shows the best electrochemical performance (discussed later). By characterizing the electrochemical performance of rGO(1%)/$AlPO_4$(1%)-coated LMNO electrode, we want to confirm that all of the rGO/$AlPO_4$-coated electrodes could be potential candidates for the advanced 5 V spinel cathode materials for Li-ion batteries as well. Thus, the LMNO electrodes before and after surface modification with rGO(1%)/$AlPO_4$ (1%) are cycled at higher current rates of 1 C and 10 C as illustrated in Figure 5. In the case of pristine LMNO electrode, it delivers a capacity of 98 mAh g^{-1} at 80 cycles and at 1 C, which corresponds to a capacity retention of 76%. On the other hand, rGO(1%)/$AlPO_4$(1%)-coated LMNO electrode exhibits a capacity of 124 mAh g^{-1} corresponding to a capacity retention of 99% at the same cycles and current rate. In addition, when cycled at higher current rate of 10 C, rGO(1%)/$AlPO_4$(1%)-coated LMNO electrode demonstrates stable cyclic performance, while the pristine LMNO reveals fast capacity fade as shown in Figure 5. This might be due to the incorporation of conductive rGO on the surface, which

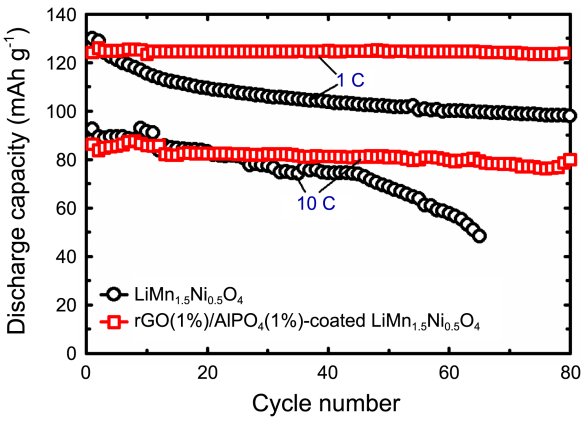

Figure 5. Cyclic performance of pristine $LiMn_{1.5}Ni_{0.5}O_4$ and rGO(1%)/$AlPO_4$(1%)-coated $LiMn_{1.5}Ni_{0.5}O_4$ electrodes at high current rates of 1 C and 10 C.

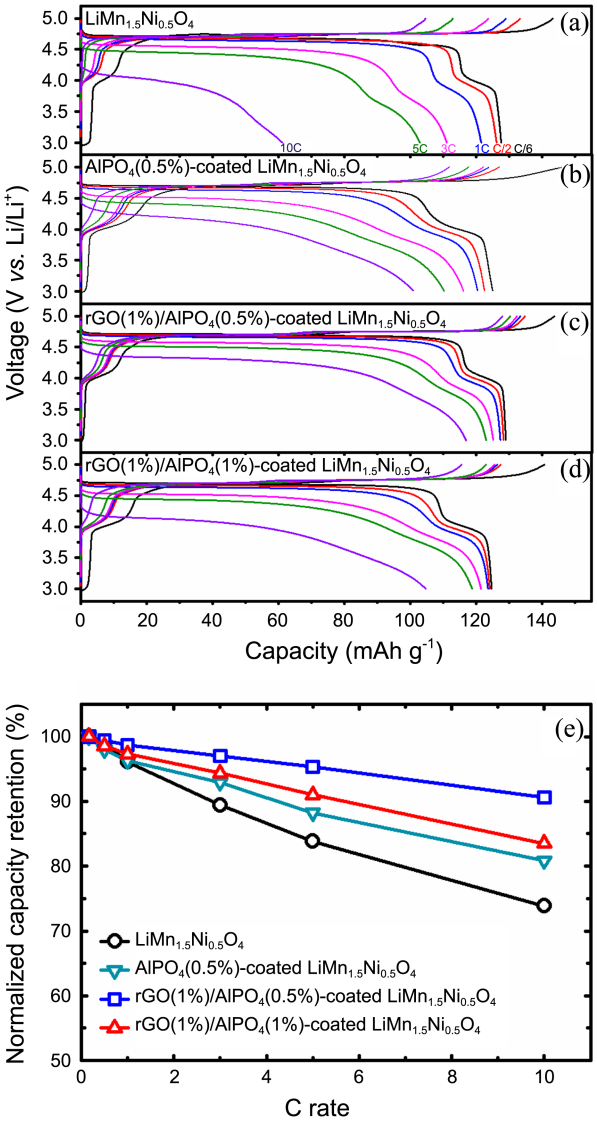

Figure 6. (a)-(d) Charge and discharge voltage profiles of pristine and surface-modified $LiMn_{1.5}Ni_{0.5}O_4$ electrodes with a constant charge rate of C/6 and various discharge rates. (e) Normalized discharge capacity values at various current rates.

increases the surface electronic conductivity of the cathode, resulting in low impedance.

Figure 6(a)-(d) compare the discharge profiles of pristine and surface-modified LMNO electrodes at various current rates. As shown in Figure 6, rGO/$AlPO_4$-coated LMNO electrodes demonstrate better rate capabilities than the pristine and $AlPO_4$-coated LMNO electrodes. Among them, the rate capability of rGO(1%)/$AlPO_4$(0.5%)-coated LMNO electrode exhibits the best rate capability. To illustrate the differences between the pristine and surface-modified LMNO samples in a better manner, the discharge capacity values at various current rates are normalized by the discharge capacity value at a C/6 rate, which is shown in Figure 6(e).

For instance, the $AlPO_4$-coated LMNO electrode exhibits a discharge capacity retention of 81% at 10 C, while the pristine LMNO electrode reveals a discharge capacity retention

of 73% at 10 C. In addition, the rGO/$AlPO_4$-coated LMNO electrodes retain a discharge capacity of 84% for rGO(1%)/$AlPO_4$(1%)-coated LMNO electrode, and 91% for rGO(1%)/$AlPO_4$(0.5%)-coated LMNO electrode at 10 C rate. Therefore, the rate capabilities decrease in the following order: rGO(0.5%)/$AlPO_4$(1%) > rGO(1%)/$AlPO_4$(1%) > $AlPO_4$ (0.5%) > pristine sample.

Polarization resistance could act as a significant role regarding the rate-capability.[26] In order to explore a relation between the rate-capability and the total polarization resistance (R_p), the discharge profiles at various discharge current rates were analyzed for the pristine, $AlPO_4$-, and rGO/$AlPO_4$-coated LMNO electrodes. The R_p value consists of the polarization resistances of the LMNO cathode and the Li foil anode, the separator resistance, and the electrolyte resistance. It can be assumed that the polarization resistance coming from Li foil anode, separator, and electrolyte is identical as same Li foil, separator, and electrolyte are utilized for all cells. Therefore, the R_p value obtained here is capable of being used as an index to compare the polarization resistance between the pristine and surface-modified LMNO electrodes. The R_p value can be obtained from the voltage −current curve (V−I) in the domain showing a linear relationship between V and I. In the case of pristine and surface-modified LMNO, the linear domain ranges (data not shown) from 10% to 60% depth of discharge (DOD), from which the R_p values is able to be extracted from the slopes of these curves. Figure 7 demonstrates the R_p values as a function of DOD for the pristine, $AlPO_4$-, and rGO/$AlPO_4$-coated LMNO samples. The R_p values increase with increasing DOD, illustrating that the kinetics of the discharge reaction becomes more unfavorable during the Li-insertion process. In addition, the pristine LMNO electrode reveals the highest R_p value at a given DOD when compared to the surface-modified LMNO electrodes.

The R_p value increases in the following order: rGO(1%)/$AlPO_4$(0.5%) < rGO(1%)/$AlPO_4$(1%) < $AlPO_4$(0.5%) < pristine LMNO. This is exactly reverse order of the rate capability. Therefore, it can be concluded that the surface-modified LMNO electrodes exhibit smaller polarization resistance than that of the pristine LMNO electrode, resulting in better rate capability.

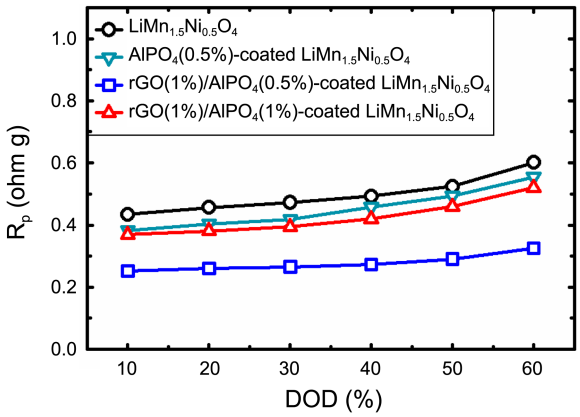

Figure 7. Variations of the polarization resistance with depth of discharge (DOD) for pristine, $AlPO_4$-, and rGO/$AlPO_4$-coated $LiMn_{1.5}Ni_{0.5}O_4$ electrodes.

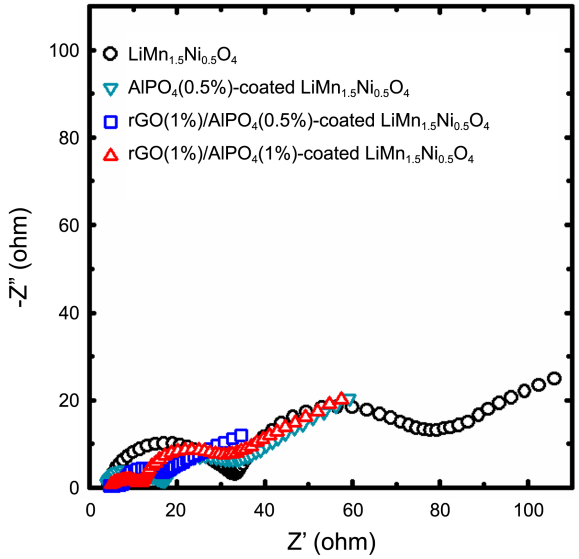

Figure 8. Electrochemical impedance spectra (EIS) of $LiMn_{1.5}Ni_{0.5}O_4$ before and after surface modification with $AlPO_4$ and rGO/$AlPO_4$ after 100 cycles.

Figure 8 compares the EIS spectra of the pristine, $AlPO_4$-, and rGO/$AlPO_4$-coated LMNO after 100 cycles. Each spectrum reveals two semicircles and a slope. The semicircle at high frequency region corresponds to the lithium-ion diffusion through the surface layer, the second semicircle at medium-to-low frequency region is related to the charge transfer reaction, and the slope at the low frequency region represents the lithium-ion diffusion in the bulk material.

The intercept of the first semicircle with the real axis corresponds to the ohmic resistance, and the diameter of the second semicircle is related to the charge transfer resistance. When observing the first- and second-semicircle at high and medium frequency regions, the pristine LMNO reveals a significant large value in SEI film resistance (R_s) and charge transfer resistance (R_{ct}) after 100 cycles. On the other hand, surface-modified LMNO electrodes demonstrate much smaller resistances than those for the pristine LMNO electrode. Specifically, rGO(1%)/$AlPO_4$(0.5%)-coated LMNO electrode demonstrates the smallest resistances after 100 cycles, as seen in Figure 8. The smaller resistances of the surface-modified LMNO electrodes might be ascribed to the suppression of thick solid-electrolyte interfacial (SEI) layer formation and better electronic conductivity when the cathode surface is modified with rGO/$AlPO_4$. In addition, at the low frequency region in the EIS spectra, the slope angles of the pristine and surface-modified LMNO samples is similar, illustrating that the lithium-ion diffusion in electrodes before and after surface-modification is conducted in a similar manner. The result of EIS measurement confirms that the rGO/$AlPO_4$-coated LMNO samples exhibit the better cyclic performance and higher-rate capability as discussed in earlier.

Conclusion

rGO/$AlPO_4$-coated $LiMn_{1.5}Ni_{0.5}O_4$ spinel cathode has been developed *via* a facile solution-based coating method. Due to the electrostatic interaction between graphene oxide surface with negative charge and Al^{3+} with positive charge resulting from the addition of aluminum nitrate nonahydrate ($Al(NO_3)_3{\cdot}9H_2O$) and then the addition of ammonium phosphate ($(NH_4)_2HPO_4$), $AlPO_4$ nanoparticles could be anchored on graphene oxide sheet. The reduction of graphene oxide was conducted during an annealing process; thus, there is no need to introduce toxic reducing agents. The surface-modification of $LiMn_{1.5}Ni_{0.5}O_4$ samples with rGO/$AlPO_4$ hybrid coating lead to better cyclic performance as well as higher-rate capability compared to those of pristine and $AlPO_4$-coated $LiMn_{1.5}Ni_{0.5}O_4$ spinel cathode. rGO/$AlPO_4$-coated $LiMn_{1.5}Ni_{0.5}O_4$ samples exhibit lower total polarization resistance, and smaller surface resistance and charge-transfer resistance, which confirms the surface-modified $LiMn_{1.5}Ni_{0.5}O_4$ spinel electrodes demonstrate enhanced electrochemical performance. Therefore, the surface modification with rGO/$AlPO_4$ hybrid coating for the $LiMn_{1.5}Ni_{0.5}O_4$ spinel presented here can be a promising approach to generate high-power cathode material for lithium-ion batteries.

Acknowledgments. This research was supported by the Gachon University research fund of 2014 (GCU-2014-0122).

References

1. Kim, T. H.; Park, J. S.; Chang, S. K.; Choi, S.; Ryu, J. H.; Song, H. K. *Adv. Energy Mater.* **2012**, *2*, 860.
2. Kim, J. S.; Vaughey, J. T.; Johnson, C. S.; Thackeray, M. M. *J. Electrochem. Soc.* **2003**, *150*, A1498.
3. Strobel, P.; Palos, A. I.; Anne, M.; Cras, F. L. *J. Mater. Chem.* **2000**, *10*, 429.
4. Zhong, Q. M.; Bonakdarpour, A.; Zhang, M. J.; Gao, Y.; Dahn, J. R. *J. Electrochem. Soc.* **1997**, *144*, 205.
5. Amine, K.; Tukamoto, H.; Yasuda, H.; Fujita, Y. J. *J. Power Sources* **1997**, *68*, 604.
6. Kraytsberg, A.; Ein-Eli, Y. *Adv. Energy Mater.* **2012**, *2*, 922.
7. Mukerjee, S.; Yang, X. Q.; Sun, X.; Lee, S. J.; McBreen, J.; Ein-Eli, Y. *Electrochim. Acta* **2004**, *49*, 3373.
8. Noguchi, T.; Yamazaki, I.; Numata, T.; Shirakata, M. *J. Power Sources* **2007**, *174*, 359.
9. Sun, Y. K.; Hong, K. J.; Prakash, J.; Amine, K. *Electrochem. Commun.* **2002**, *4*, 344.
10. Fey, G. T. K.; Lu, C. Z.; Kumar, T. P. *J. Power Sources* **2003**, *115*, 332.
11. Park, S. H.; Oh, S. W.; Myung, S. T.; Sun, Y. K. *Electrochem. Solid-State Lett.* **2004**, *7*, A451.
12. Alcantara, R.; Jaraba, M.; Lavela, P.; Tirado, J. L.; Zhecheva, E.; Stoyanova, R. *Chem. Mater.* **2004**, *16*, 1573.
13. Prabakar, S. J. R.; Han, S. C.; Singh, S. P.; Lee, D. K.; Sohn, K. S.; Pyo, M. *J. Power Sources* **2012**, *209*, 57.
14. Lee, D. K.; Han, S. C.; Ahn, D.; Singh, S. P.; Sohn, K. S.; Pyo, M. *Acs Applied Materials & Interfaces* **2012**, *4*, 6841.
15. Rao, C. V.; Reddy, A. L. M.; Ishikawa, Y.; Ajayan, P. M. *Acs Appl. Mater. Interfaces* **2011**, *3*, 2966.
16. Ban, C.; Li, Z.; Wu, Z.; Kirkham, M. J.; Chen, L.; Jung, Y. S.; Payzant, E. A.; Yan, Y.; Whittingham, M. S.; Dillon, A. C. *Adv. Energy Mater.* **2011**, *1*, 58.
17. Prabakar, S. J. R.; Hwang, Y. H.; Lee, B.; Sohn, K. S.; Pyo, M. *J. Electrochem. Soc.* **2013**, *160*, A832.
18. Stoller, M. D.; Park, S.; Zhu, Y.; An, J.; Ruoff, R. S. *Nano Lett.* **2008**, *8*, 3498.
19. Geim, A. K.; Novoselov, K. S. *Nat. Mater.* **2007**, *6*, 183.
20. Cho, J.; Kim, Y. W.; Kim, B.; Lee, J. G.; Park, B. *Angewandte Chemie-International Edition* **2003**, *42*, 1618.
21. Hummers, W. S.; Offeman, R. E. *J. Am. Chem. Soc.* **1958**, *80*, 1339.
22. Jung, K. H.; Kim, S. B.; Park, Y. J. *Journal of the Korean Electrochemical Society* **2011**, *14*, 77.
23. Wang, G.; Shen, X.; Yao, J.; Park, J. *Carbon* **2009**, *47*, 2049.
24. Talyosef, Y.; Markovsky, B.; Salitra, G.; Aurbach, D.; Kim, H. J.; Choi, S. *J. Power Sources* **2005**, *146*, 664.
25. Yi, T.-F.; Xie, Y.; Zhu, Y.-R.; Zhu, R.-S.; Ye, M.-F. *J. Power Sources* **2012**, *211*, 59.
26. Delacourt, C.; Laffont, L.; Bouchet, R.; Wurm, C.; Leriche, J. B.; Morcrette, M.; Tarascon, J. M.; Masquelier, C. *J. Electrochem. Soc.* **2005**, *152*, A913.